Effect of Power Converter on Condition Monitoring and Fault Detection for Wind Turbine

Raed Khalaf Ibrahim and Simon Watson
Centre for Renewable Energy Systems Technology (CREST),
School of Electronic, Electrical and Systems Engineering,
Loughborough University, UK
R.Ibrahim@lboro.ac.uk, S.J.Watson@lboro.ac.uk

***Abstract*—This paper investigates the impact of power electronics converter when attempting wind turbine condition monitoring system and fault diagnosis by the analysis of fault signatures in the electrical output of the turbine. A wind turbine model has been implemented in the MATLAB/Simulink environment. Fault signature analysis for electrical signals is presented. A signal processing algorithm based on a fast fourier transform is then used to potentially identify fault signatures. The results obtained with this model are validated with experimental data measured from a physical test rig. Through comparison between simulation data and experimental data it is concluded that the power converter has significantly reduced fault signatures from the electrical signal though not entirely extinguished them. It may still be possible to extract some fault information after the converter though this is much more challenging than upstream. Further work is needed to see whether it may be possible to modify the power converter particularly the filter design and the switching elements to avoid removing fault signatures from electrical signals without adding significant cost or compromising performance.**

***Index Terms*—Wind turbine, Power converter, Condition monitoring, Fault signature, Fault detection.**

I. INTRODUCTION

Wind power has been one of the fastest growing power sources in the world over the last two decades, growing from a tiny 7.6 GW in 1997 to 370 GW in 2014 [1]. The worldwide wind capacity reached 392.927 GW by the end of June 2015, out of which 21.6 GW were added in the first six months of 2015. This increase is substantially higher than in the first half of 2014 and 2013, when 17.6 GW respectively 13.9 GW were added. All wind turbines (WTs) installed worldwide by mid-2015 can generate 4 % of the worlds electricity demand [2].

WT manufacturers have been considering induction or synchronous generators with fully rated power converters to give full- power and variable-speed operation. In this case the electrical power from WTs is transferred through the power converter so that the influence of the power converter on a WT condition monitoring and fault diagnosis system which is specifically monitoring the electrical signals has to be thoroughly investigated. The signature of electrical signals has been widely applied for diagnosis of both electrical and mechanical faults of electrical machines in conventional generation plants. There are several advantages that monitoring the electrical signals offers when compared to other condition monitoring methods. For example, electrical analysis can provide a reliable indication of the presence of a fault for the monitored system; it can indicate the location and severity of the fault; it can give immediate information about the state of health of that system [3], where in contrast with oil analysis, several days elapse between the sample collection and their analysis. Moreover, where in contrast with oil analysis, several days elapse between the sample collection and their analysis. Moreover, the main driver for using electrical signals is to reduce costs given that the electrical current and voltage are continuously measured [4]. Thus, monitoring the electrical signals has gained more attention from researchers and industry for WT condition monitoring and fault diagnosis. However, there are still challenges in analysing fault signatures from the electrical signals of WTs. For example, the useful information in electrical signals has nonlinear and non-stationary characteristics due to the constantly varying loads, the variable speed nature of most WTs, the nonlinear operation of the machines, the presence of power electronics and the low signal to noise ratio of measured potential fault signals.

In this paper, the impact of the the power converter on fault signature in WT electrical signals is investigated. This has been done by creating a WT model in MATLAB. The results obtained with this model are compared with experimental data measured from a physical test rig at Durham University. A signal processing algorithm based on a fast fourier transform (FFT) is then used to compare the electrical signature of both a healthy and a faulty WT.

II. EFFECT OF POWER CONVERTER ON ELECTRICAL SIGNALS

The AC power system which is operating normally has a current and voltage waveform which is varying sinusoidally at a specific frequency. In other words, a linear electrical load draws sinusoidal current at the same frequency as the voltage when it is connected to the power system (though usually not in phase with the voltage). With the increase in use of power converters and other switching devices which are considered as non-linear loads. Non-linear loads are mainly considered

as harmonic sources because non-linear loads consume only some part of the sinusoidal current and voltage rather than consuming the full wave. This distortion in the current and voltage waveforms will cause unwanted harmonics. It has been reported in [5] that high levels of harmonic distortion can be caused by components such as capacitors, static VAR compensators, inverters, AC converters, switch-mode power supplies, AC or DC motor drives, etc. However, the use of power electronic equipment with switching always leads to harmonic disturbances causing power quality issues in the grid [6].

Generally, the power produced from a WT with a fully rated con-verter is first converted into DC and then converted back to AC with the grid frequency. On the DC side, the harmonics are of less importance, because the DC load acts as a filter with highly inductive impedance, which minimizes the level of harmonics. Since the DC harmonic is within the zero sequence, there is no transfer of these harmonics between the different voltage levels. While on the AC side, the AC filters are used to minimize the flow of harmonic current into the AC network. There are two types of AC harmonic filters: tuned filter and high pass filter [7]. In a large AC/DC power converter, two or more tuned filters are employed for the lower-harmonic (one for each harmonic frequency). These filters are used in the reduction of harmonic currents in the AC-side of the converter. Furthermore, the power converters inject harmonic currents or voltages into the power system in order to control the steady-state and dynamic active and reactive power [8].

In these investigations, it is found that power converters have clearly effected the electrical signals by either minimizing the harmonics level or adding harmonics into the electrical signals, meaning that any fault signature in electrical signals might be effected as well. In order to have a more clear understanding of the effect of the power converter on the faults signature, it is essential to understand the analysis of the fault signature of that electrical signal.

III. FAULT SIGNATURE ANALYSIS FOR ELECTRICAL SIGNALS

Voltage and current are electrical signals which can be acquired from the terminals of electrical machine such as generators and motors. The signature of electrical signals has been widely applied for diagnosis of both electrical and mechanical faults of electrical machines in nuclear, fossil-fuel and hydro power stations. Stator current analysis for WT fault detection has been in practice for quite some time now, for further details, see [9]. However, if a fault occurs in a WT this might cause radial rotor movement and shaft torque variation of the WT. Accordingly, these fault effects will modulate the amplitude and frequency of the current signals measured from the terminals of the generator. If we suppose $i(t)$ be the instantaneous current signal of a healthy WT, then the fundamental component waveform of $i(t)$ is

$$i(t) = I_{max} \sin(2\pi f t + \phi) \tag{1}$$

where t is the time index in second; f is the fundamental frequency (50_{Hz} or 60_{Hz}), I_{max} and ϕ are the amplitude, frequency and phase of the fundamental component of the current signal, respectively. It is clear from a power system point of view that current signals may include more or less higher harmonic components for various reasons. Harmonics can be defined as waveforms superimposed on a fundamental waveform having frequencies different to the fundamental frequency. The frequency of each harmonic component is known as the harmonic frequency. The harmonic component of a current of order n can be represented by using Fourier series as

$$i_h^n(t) = I_n \sin(2\pi n f t + \phi) \tag{2}$$

where n is the harmonic order, and I_n is the amplitude of harmonic component. Generally, the current signal will be as follows:

$$i(t) = I_{max} \sin(2\pi f t + \phi) + i_h^n(t) \tag{3}$$

It is assumed below that $i_f(t)$ is the current signal for a faulty WT

$$i_f(t) = I_f \sin(2\pi f_f t + \phi_f) + \bar{i}_h^n(t) \tag{4}$$

where I_f, f_f, ϕ_f and $\bar{i}_h^n$ are the amplitude, frequency, phase and harmonics of the current signal during fault conditions, respectively. It is important to highlight that the main driver for the analysis of the current signal is to detect I_f), f_f, ϕ_f and $\bar{i}_h^n(t)$, which are the signatures of the WT fault in the current signal. But, as mentioned before, signal to noise ratio of measured signals (current and voltage) is low. Accordingly, the traditional methods based on time domain analysis cannot easily uncover the characteristics of time-varying components. In order to have a more clear understanding of the characteristics of the fault current signal in (4), the techniques of amplitude, frequency and phase modulation, used in electronic communication (see [10] for details), will be adopted in this research. Consequently, the modulated current signal i_m of the fault current signal in (4) can be modeled as:

$$i_m(t) = I_{peak} \sin(2\pi f_m t + \phi_m) + \gamma \tag{5}$$

where I_{peak}, f_m, ϕ_m are the current components due to amplitude modulation, frequency modulation and phase modulation generated by WT faults, respectively; γ represents the harmonics and other excitations of the current signal during fault events. Figure 1 shows a current waveform during an asymmetrical fault. It can be clearly seen how the current signals has been modulated onto the fault signal.

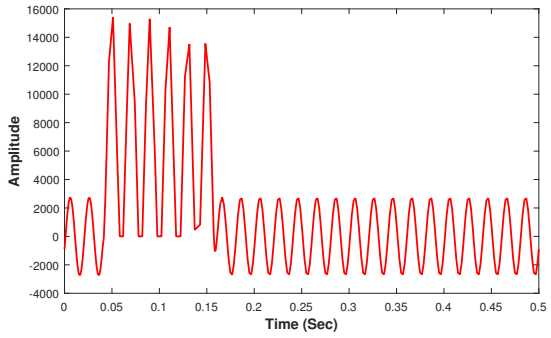

Fig. 1: Current signal during fault events

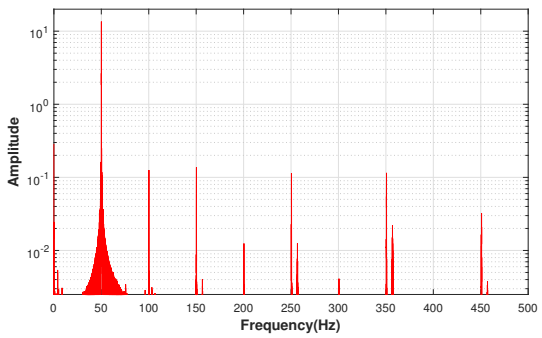

Fig. 2: Non-sinusoidal complex waveforms in frequency domain

To overcome the shortcomings of time domain analysis, technique such as fourier transform is used for feature extraction. The fourier transform is can be used to convert the time description of the continuous waveform $x(t)$ into an equivalent function in frequency by:

$$X(f) = \int_{-\infty}^{\infty} x(t) e^{-j2\pi ft}\, dt \tag{6}$$

Then, Eq. (5) can be rewritten as:

$$F[I_m(f)] = \int_{-\infty}^{\infty} i_m(t) e^{-j2\pi ft}\, dt \tag{7}$$

substituting Equation (5) into Equation (7) and neglecting the phase term,

$$F[I_m(f)] = \int_{-\infty}^{\infty} [I_{peak} \sin(2\pi f_m t) + \gamma] e^{-j2\pi ft} dt \tag{8}$$

while

$$\sin 2\pi ft = \frac{e^{j2\pi ft}}{j2} - \frac{e^{-j2\pi ft}}{j2} \tag{9}$$

then by manipulation to obtain the following equation:

$$F[I_m(f)] = \frac{1}{j2} I_{peak}[\delta(f + f_m) - \delta(f - f_m)] + H_f \tag{10}$$

Here $F[I_m(f)]$, H_f represent the modulated current signal and the harmonics in the frequency domain, respectively. In these investigations, it is found that the fourier transform of a sinusoidal waveform can be considered as a train of impulses as shown in Figure 2.

IV. SIMULATION AND EXPERIMENTAL TOOLS

A. Test Rig

The effect of the power converters on fault signatures has been validated using experimental data measured from a physical test rig kindly offered by the staff at Durham University. The test rig consisted of a 50-kW DC variable-speed drive connected via a 5:1 gearbox to a four-pole doubly fed induction generator (DFIG) connected as a wound rotor induction generator as shown in Figure 3. The test rig is described in more detail in [11]. The effect of rotor electrical asymmetry on DFIG steady-state current was investigated on the test rig. Tests were first performed for a typical on-line operating point of 1550 rpm with balanced windings and a load torque of 20 Nm. The measured supply frequency was 51.27 Hz in the experiments. Additional resistance was then introduced in one rotor phase to emulate fault conditions and stator line currents were recorded.

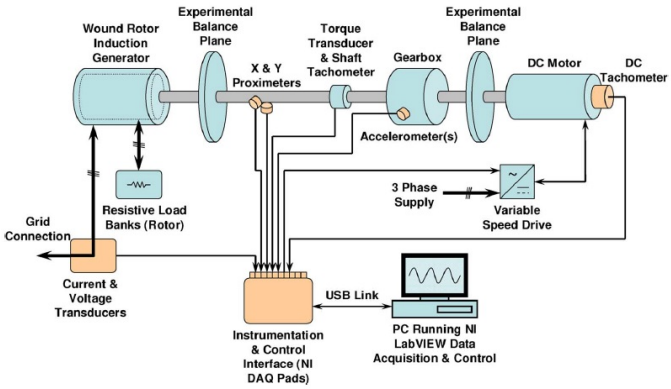

Fig. 3: Schematic presentation of the test rig [12]

B. Mathematical Model of Test Rig

In this work, we developed a mathematical model for the test rig at Durham University, and then we used their measured data to validate the model. The mathematical representation of the Test Rig can be divided into three fundamental models:

- Wind speed, Rotor and Pitch control model used to represent the DC motor and controller in the physical Test Rig which was used to create a torque on the system;
- Drive-train model, which represents the inertia of the DC motor, gearbox and generator, and also the damping, stiffness of gearbox and speed shafts.
- Electrical model including the generator electrical part, power converter and grid.

1) Wind Speed Model: This model is used to generate short-term wind speed variations with certain characteristics, such as speed range or turbulence intensity, which a WT will experience. The wind speed v_w is modeled as the sum of the four components [13].

$$v_w(t) = v_{avg} + v_r(t) + v_g(t) + v_n(t) \tag{11}$$

where v_{avg} is the average value of the wind speed, $v_r(t)$ is a ramp wind speed component, $v_g(t)$ is the gust wind speed component and $v_n(t)$ is the base noise wind speed component (turbulence).

2) Rotor Model: The rotor transfers the kinetic energy from the wind into mechanical energy at the rotor shaft by aerodynamic forces producing lift on the blades. The kinetic energy of a cylinder of air of radius R traveling with wind speed v_w corresponds to a total wind power P_w within the rotor swept area of WT. The WT mechanical power output can be defined as :

$$P_w = \frac{1}{2}\rho\pi R^2 v_w^3 C_P(\lambda, \beta) \tag{12}$$

where P_w is the extracted wind power; ρ is the air density (1.225 kg/m3); R is the rotor radius and V_{wind} is the wind speed; and C_P is the efficiency coefficient of the turbine which is the function of the tip-speed ratio λ and the blade pitch angle β. The tip-speed ratio λ is expressed as :

$$\lambda = \frac{\omega_t R}{v_w} \tag{13}$$

where, ω_m is the turbine rotational speed. If the mechanical torque T_t is to be applied instead of the mechanical power P_t, it can be easily calculated from the dynamic theory of rotating devices in physics by using the turbine rotational speed ω_t:

$$T_t = \frac{P_t}{\omega_t} \tag{14}$$

3) Drivetrain Model: The equivalent model of the Test Rig drive train is presented in Figure 4. The masses correspond to a large mass of the WT rotor, masses for the gearbox wheels and a mass for the generator respectively.

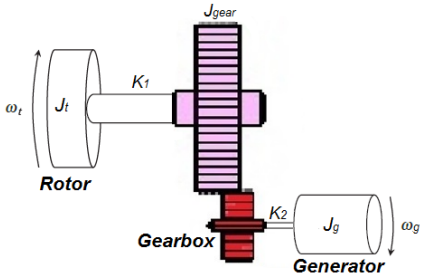

Fig. 4: Three masses model of the Test Rig drive train.

However, the moment of inertia for the shafts and the gearbox wheels can be neglected because they are small compared with the moment of inertia of the WT or generator. We therefore use a two-mass representation of the drive train by considering an equivalent system with an equivalent stiffness and damping factor. The two-mass representation is described by the equations:

$$\begin{aligned} J_t \frac{d^2}{dt^2}\theta_t &= -K(\theta_t - \theta_g), \\ J_g \frac{d^2}{dt^2}\theta_g &= -K(\theta_g - \theta_t). \end{aligned} \tag{15}$$

J_t, J_g are the moments of inertia of the turbine and generator respectively (kgm^2),ω_g is the rotational speed of the generator (rad/s), θ_t, θ_g are the rotational displacements of the turbine and generator respectively (rad), K is the shaft stiffness (Nm/rad).

4) Generator model: The generator used was a DFIG and was modelled as a 5th order system of differential equations which can be found in [14].

5) Power converter: In modern variable-speed WTs, the converter consists of a Graetz Bridge with Insulated Gate Bipolar Transistors (IGBTs) as the switching elements. The bridges are switched rapidly (typically between 2 - 6 kHz) with some form of pulse width modulation (PWM) to produce a close approximation to a sine wave. The generator converter rectifies all the power to DC, which is then inverted to AC by the network converter.

The power converter was modelled as an AC/DC/AC converter consisting of an IGBT rectifier feeding an IGBT inverter through a DC link as shown in Figure 5.

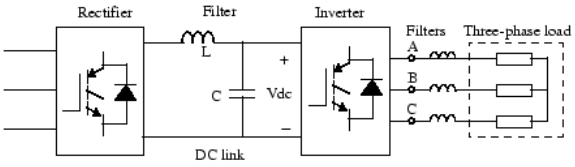

Fig. 5: Model of the power converter.

The inverter is PWM to produce a three-phase 50 Hz sinusoidal voltage to the load. In this example the inverter chopping frequency is 2000 Hz. The parameters of the power

converter were based on the power modules found in the SEMIKRON [15]. The simulation results for the line current of the rectifier and inverter model are given in Figure 6. The results clearly show that the power converter has added harmonics into the line current which are then removed by the filter.

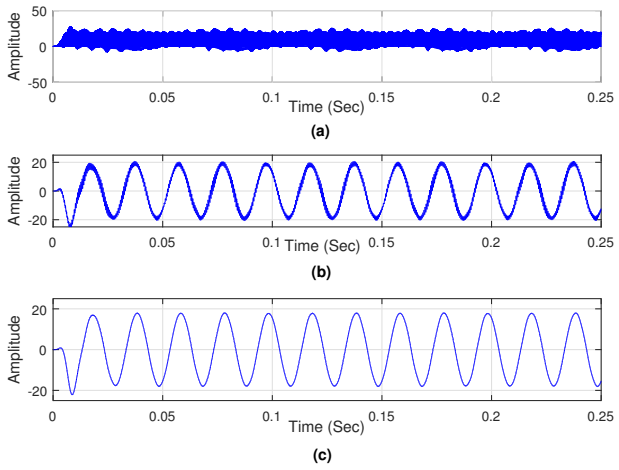

Fig. 6: The line current of (a) rectifier (b) inverter-side before the filter and (c) after the filter.

V. RESULTS AND DISCUSSIONS

The model of the WT during steady-state operation is validated against measurements on the Test Rig. Figure 7 shows the measured and simulated signal in the time domain for the line current obtained before the converter. The good agreement between the results obtained with both the Test Rig and the corresponding model permits us to study the effects of the power converter on the fault signature. As mentioned before, the traditional methods based on time domain analysis cannot easily uncover the characteristics of the harmonics. Therefore, a signal processing algorithm based on FFT is used to convert the line current signal from time domain into frequency domain in order to extract features of harmonics related superimposed on the fundamental frequency. The line current spectra, before and after the converter, are compared for signature analysis during the steady-state as shown in Figure 8 and Figure 9. It is clear that the line current spectrum after the converter for both measured and simulated data has different characteristics and more harmonics compared to the results before the converter. This is mainly because the rectifier and the filter have removed all the harmonic frequencies during the conversion from AC to DC, and also because of the switching elements that are inherent in the operation of the inverter so that new harmonic components are injected into the reference waveform. It is important to mention that the converter at Durham University had a fault at the time of preparation were of this paper. Therefore, the experimental data has been simulated and then applied to the power converter model in order to investigate the effects of the power converter on fault signatures from the measured data from the Test Rig.

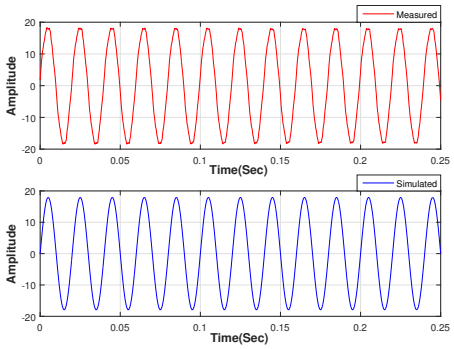

Fig. 7: Line current obtained before the converter for healthy measured data and healthy simulated data.

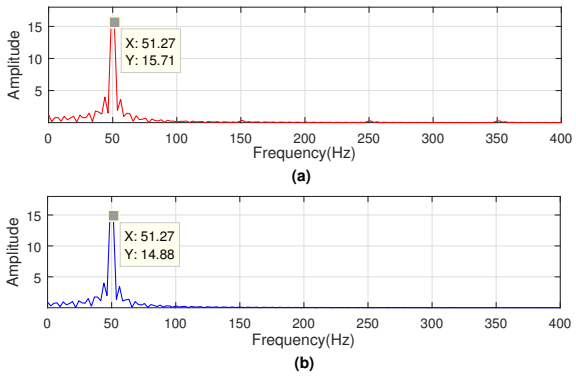

Fig. 8: Line current spectra obtained before the converter for (a) healthy measured data and (b) healthy simulated data.

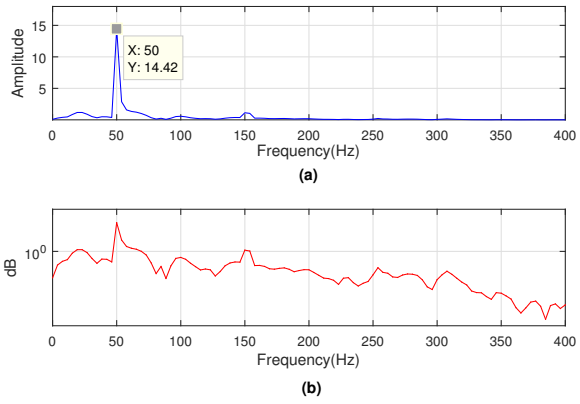

Fig. 9: Line current obtained after the converter for healthy simulated data as (a) spectrum and (b) power distribution density.

A case study is presented in this work in order to investigate the effect of the power converter on fault signature analysis.

The effect of rotor electrical asymmetry on the line current of the test rig was investigated. Figure 10 shows the spectrum of the line current for a faulty WT acquired before the converter. The results clearly indicate that rotor unbalance induces a change of considerable magnitude in a number of frequencies in the current and power spectra. These sidebands have been shown to be most pronounced at the third, the fifth and the seventh harmonic of the supply frequency. These harmonics are an indication of the presence of the fault. While in Figure 10, it is more difficult to extract information to be sure of a fault although the 5^{th} and 7^{th} harmonics are still just visible. This is mainly due to the presence of the DC filter, the AC filter and the switching elements that are inherent in the operation of the inverter which are used with the power converter to eliminate undesired harmonics and DC components. This indicates that fault diagnosis after the converter is not impossible though more challenging than before the converter.

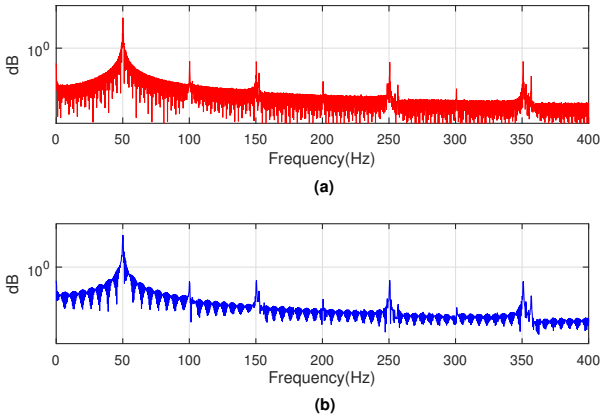

Fig. 10: Power spectrum density for line current obtained before the converter for (a) faulty measured data and (b) faulty simulated data.

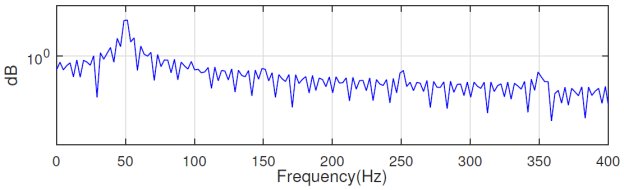

Fig. 11: Power spectrum density for line current obtained after the converter for faulty simulated data.

VI. Conclusion

In this work, the effects of power converters on fault diagnosis through analysis of the electrical signature is presented. This has been done by implementing a WT model using Matlab/Simulink. The model was able to adequately represent the behaviour of the power converter and its effect on the WT condition monitoring system and fault diagnosis through the stator current signature. The results obtained with this model are compared with experimental data measured from a physical test rig. An FFT algorithm was then used to compare the electrical signature of a healthy and faulty WT to observe how the features would appear in the fault detection and diagnosis methods. Both the simulation and experimental results show that the fault signature has been diminished by either minimizing the harmonic levels through the rectifier or by adding harmonics into the electrical signals by the inverter so that the useful information in current measurements that could be used for WT condition monitoring and fault detection has a low signal to noise ratio, which makes the condition monitoring and fault detection more difficult. Ultimately, the results of this research could be used for future studies to see how much fault information could still be extracted after the converter to modify the power converter by such as changes to the filter design and the switching elements to avoid removing faults signature from the electrical signals without significant extra cost or compromising of performance.

References

[1] Global Wind Energy Counci, Global Cumulative Installed Capacity 1997-2014, [Online]: http://www.gwec.net/global-figures/graphs/, 2014.

[2] The World Wind Energy Association, WWEA BULLETIN SPECIAL ISSUE 2015, [Online]: http://www.wwindea.org/wwea-bulletin-special-issue-2015/.

[3] P. Zhang and P. Neti, "Detection of gearbox bearing defects using electrical signature analysis for Doubly-fed wind generators," *2013 IEEE Energy Conversion Congress and Exposition*, pp. 4438–4444, Sept. 2013.

[4] J. P. Barton and S. J. Watson, "Analysis of electrical power data for condition monitoring of a small wind turbine," *IET Renewable Power Generation*, vol. 7, no. 4, pp. 341–349, 2013.

[5] R. G. Ellis, "A reference guide to causes, effects and corrective measures," *Power systems harmonics, Rockwell International Corporation, Canada*, 2001.

[6] N. Mohan and T. M. Undeland, *Power electronics: converters, applications, and design*. John Wiley & Sons, 2007.

[7] S. Talib, S. Bashi, and N. Mailah, "Simulation and analysis of power converter harmonics," in *Research and Development, 2002. SCOReD 2002. Student Conference on*, pp. 213–216, IEEE, 2002.

[8] Z. Chen, J. M. Guerrero, and F. Blaabjerg, "A review of the state of the art of power electronics for wind turbines," *Power Electronics, IEEE Transactions on*, vol. 24, no. 8, pp. 1859–1875, 2009.

[9] W. Yang, P. J. Tavner, C. J. Crabtree, and M. Wilkinson, "Cost-effective condition monitoring for wind turbines," *Industrial Electronics, IEEE Transactions on*, vol. 57, no. 1, pp. 263–271, 2010.

[10] H. Simon S, *Introduction to analog and digital communications*. Hoboken, NJ : Wiley, 2007.

[11] M. R. Wilkinson, F. Spinato, and P. J. Tavner, "Condition monitoring of generators & other subassemblies in wind turbine drive trains," in *Diagnostics for Electric Machines, Power Electronics and Drives, 2007. SDEMPED 2007. IEEE International Symposium on*, pp. 388–392, IEEE, 2007.

[12] W. Yang, P. Tavner, C. Crabtree, and M. Wilkinson, "Cost-effective condition monitoring for wind turbines," *Industrial Electronics, IEEE Transactions on*, vol. 57, pp. 263–271, Jan 2010.

[13] P. Anderson and A. Bose, "Stability simulation of wind turbine systems," *Power Apparatus and Systems, IEEE transactions on*, no. 12, pp. 3791–3795, 1983.

[14] V. Akhmatov, "Variable-speed wind turbines with doubly-fed induction generators, part i: Modelling in dynamic simulation tools," *Wind Engineering*, vol. 26, no. 2, pp. 85–108, 2002.

[15] SEMIKRON, 3-phase bridge rectifier +3-phase bridge inverter SK 20 DGD 065 ET, [Online]: http://http://www.semikron.com/dl/service-support/downloads/download/semikron-datasheet-sk-20-dgd-065-et-24910430.